

Simple and efficient decoupling in magic-angle spinning solid-state NMR: the XiX scheme

Andreas Detken, Edme H. Hardy¹, Matthias Ernst, Beat H. Meier^{*}

Physical Chemistry, ETH-Zurich, CH-8093 Zurich, Switzerland

Received 13 December 2001

Abstract

We propose a simple heteronuclear decoupling scheme for spin-1/2 nuclei under magic-angle sample spinning (MAS). The sequence, called XiX, consists of windowless rf irradiation with a repeat of two pulses of equal width, phase-shifted by 180°. The XiX scheme is found to be, within certain limits, insensitive to the flip angle of the individual pulses but only sensitive to the pulse width in units of the rotor period. It is therefore easier to implement and optimize than previously used sequences. The new sequence can lead to a significant improvement in decoupling over published sequences, in particular at high MAS frequencies. © 2002 Published by Elsevier Science B.V.

1. Introduction

In carbon-13 or nitrogen-15 NMR, spin decoupling from the protons is a prerequisite for obtaining high spectral resolution. In liquid-state NMR, efficient decoupling schemes are well established, and the resolution is usually limited by relaxation effects. In solid-state NMR under rapid magic-angle sample spinning (MAS), the relaxation-limited linewidth would often be very narrow, but important other sources of line broadening exist and dominate the linewidth. A

significant contribution to the linewidth originates from the heteronuclear dipolar interactions with the protons. Efficient averaging of these interactions by a decoupling sequence is therefore mandatory. This is addressed in the present work.

Only in the last few years, decoupling pulse sequences that outperform continuous-wave (cw) decoupling [1–3] in solids have been developed. Today, the most widely used decoupling sequence is two-pulse phase-modulated (TPPM) decoupling [4] which can lead to strongly reduced linewidths compared to cw decoupling. A similar performance as for TPPM has been achieved with other recent decoupling sequences, such as FMPM [5], C12₂⁻¹ [6], SPARC [7] and SPINAL [8], or amplitude-modulated TPPM [9].

TPPM involves a continuous irradiation of the protons with a repeat of two pulses of equal flip angle α_p , usually close to π , and with a rf-phase

^{*} Corresponding author. Fax: +41-1-632-1621.

E-mail address: beat.meier@nmr.phys.chem.ethz.ch (B.H. Meier).

¹ Present address: Institut für Mechanische Verfahrenstechnik und Mechanik, Universität Karlsruhe, D-76128 Karlsruhe, Germany.

difference of $\Delta\phi$, typically in the range of 10° – 70° . The performance of TPPM depends strongly on the flip angle α_p and on the phase difference $\Delta\phi$, the dependence becoming more pronounced at high MAS frequencies. Therefore, both α_p and $\Delta\phi$ must be optimized experimentally in order to achieve optimum performance of the sequence. The optimum values vary between different samples and MAS frequencies. The pronounced sensitivity to the flip angle $\alpha_p = 2\pi\nu_1 t_p$ translates, for a fixed pulse width t_p , into a strong susceptibility to rf instability and inhomogeneity.

In this contribution, we propose a simple high-power decoupling scheme which, in many instances, leads to a significant improvement in decoupling performance compared to TPPM and other published sequences. For low-power decoupling, different design principles apply [10]. The new scheme, sketched in Fig. 1a, consists of con-

tinuous irradiation of the protons with pulses of equal width t_p and with a phase difference of 180° . We call this sequence XiX (X inverse-X). Technically, the sequence corresponds to TPPM with a phase angle $\Delta\phi = 180^\circ$. However, completely different considerations apply for the choice of the pulse width t_p . For TPPM, the flip angle, i.e. the product of the pulse width t_p and the rf-field amplitude ν_1 is decisive for the performance (in addition to the phase angle $\Delta\phi$). For XiX, the performance depends, to a good approximation, only on the pulse width t_p in units of the rotor period $\tau_r = 1/\nu_r$, i.e., synchronization with the MAS rotation is the only experimental setting. Experimental optimization of the new sequence is considerably simpler because it only concerns a single parameter, t_p/τ_r . This parameter is particularly easy to control by the experimentalist. Based solely on the MAS frequency, a good initial value for the pulse width t_p can be predicted. For optimum performance, some fine tuning of this value is still needed as the optimum pulse width is not entirely independent of the sample and the MAS frequency. This dependence is, however, much weaker than for TPPM.

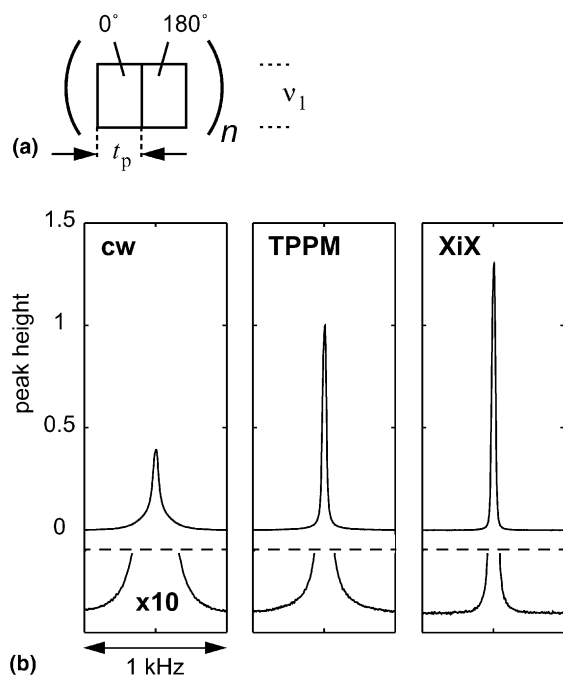


Fig. 1. (a) Sketch of the XiX sequence. The protons are irradiated continuously with pulses of equal width t_p and opposite phase. (b) The C^{13} resonance of alanine under different decoupling schemes at an rf-field amplitude of $\nu_1 = 150$ kHz. The MAS frequency was 30.03 kHz. (Left) cw decoupling; (center) optimized TPPM decoupling ($t_p = 3.1$ μ s and $\Delta\phi = 27^\circ$); (right) optimized XiX decoupling ($t_p = 94.9$ μ s).

2. Materials and methods

Experiments were performed at a B_0 field of 14.09 T on a Bruker AV-600 spectrometer equipped with a Bruker 2.5 mm double-resonance MAS probe. The timing of all pulse sequences was carefully checked using a digital high-frequency oscilloscope (Tektronix TDS784D) for eliminating ‘hidden’ delays in the pulse timing. The MAS frequency was stabilized to within ± 5 Hz. APHH CP [11,12] from the protons was used for generating initial ^{13}C coherence, immediately followed by data acquisition under 1H decoupling. Experiments were performed at MAS frequencies between 10 and 30 kHz on samples of 2- ^{13}C -alanine and 2- ^{13}C -glycine. In each case, a full rotor of the 98%+ labelled material (Cambridge Isotopes Laboratory) was used unless mentioned otherwise.

Numerical simulations were performed using the C++ library GAMMA [13]. The spin system

was modeled by a dipolar-coupled I-S two-spin system which was described in Hilbert space. The following parameters were used for the simulation: anisotropy of the dipolar coupling $\delta_D = 46$ kHz, anisotropy of the symmetric I-spin CSA $\delta_I = 3$ kHz, S-spin CSA $\delta_S = 0$ kHz, rf-field amplitude $\nu_1 = 147$ kHz, MAS rotation frequency $\nu_r = 30$ kHz. The simulations were carried out with a piecewise-constant Hamiltonian, each rotor period being divided into 100 time steps. A powder average over 100 orientations was calculated. After applying a cosine-squared window function and Fourier transformation, the maximum peak height in the spectrum was extracted and used as a measure for the performance.

3. Characterization of the XiX pulse sequence

Fig. 1b compares the decoupling efficiency of the XiX decoupling scheme with TPPM and cw decoupling. The figure shows the C^α resonance of alanine for MAS at 30 kHz. For all three decoupling schemes, the same decoupling-field amplitude of 150 kHz was applied. For TPPM, both parameters t_p and $\Delta\phi$ were carefully optimized by systematically varying the TPPM pulse width t_p and the phase-modulation angle $\Delta\phi$ on a two-dimensional grid in steps of $0.1 \mu\text{s}$ and 1° , respectively. For XiX, the pulse width was optimized in steps of $0.1 \mu\text{s}$. Both TPPM and XiX are clearly superior to cw decoupling. The peak height for XiX decoupling is increased by 29% over TPPM, while the line width (FWHH) is only slightly reduced, namely from 33 Hz (TPPM) to 31 Hz (XiX). The reason for this apparent contradiction is that the broad ‘foot’ that is visible under TPPM is sharpened under XiX decoupling and now contributes to the central, narrow part of the line.

The dependence of the experimental peak height on the pulse width in XiX decoupling is shown in Figs. 2a–c for different rf-field amplitudes ν_1 and MAS frequencies ν_r . Good decoupling is achieved whenever the pulse width exceeds approximately one rotor period and unwanted ‘resonance’ conditions, where the decoupling is compromised, are avoided. For a broad range of

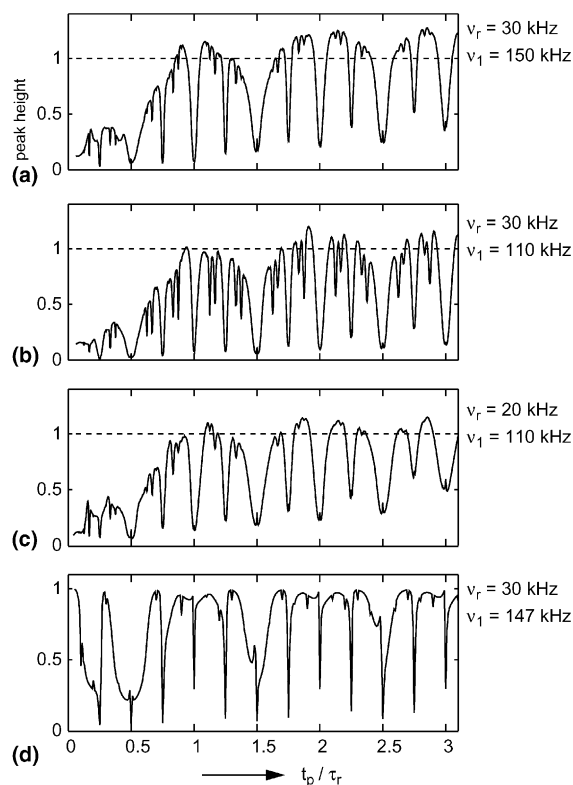


Fig. 2. (a)–(c) Dependence of the measured line height of the C^α resonance of alanine on the pulse width in XiX decoupling. The line heights are normalized to optimized TPPM decoupling at the same MAS frequencies and rf-field strengths; values >1 indicate improved performance over TPPM; (d) dependence of the simulated line height on the pulse width in XiX decoupling for an isolated two-spin system.

pulse widths t_p , the peak height of the NMR lines under XiX decoupling is higher than the optimized TPPM value, which is indicated by a dashed line. Even though there is a large number of unwanted ‘resonances’ with bad decoupling performance, fortunately their positions are largely independent of the decoupling strength and the MAS frequency (if plotted in units of the rotor period τ_r). Therefore values where a good decoupling performance is achieved can easily be predicted (vide infra).

The ‘resonances’ follow a regular pattern. The strongest ‘resonances’ occur when the pulse width approximately matches a multiple of one half of a rotor period. Around these conditions, the spec-

trum exhibits broad lines, sometimes with strong cycling sidebands. At odd multiples of a quarter rotor period, narrower, but still very deep ‘resonances’ are observed. Finally, weak ‘resonances’ are found whenever the pulse width approximately matches certain multiples of 1/24th of the rotor period. In the experimental data of Fig. 2 we find such minima for $t_p = (3n \pm 1) \cdot \tau_r/3$, $t_p = (6n \pm 1) \cdot \tau_r/6$, $t_p = (8n \pm 1) \cdot \tau_r/8$, and $t_p = (8n \pm 3) \cdot \tau_r/8$, where n is an integer. Some of these additional ‘resonances’ get more pronounced at lower rf-field amplitudes. With larger ratios t_p/τ_r , the ‘resonances’ become weaker, but the peak height at the local performance maxima between the ‘resonances’ decreases. Ultimately, the performance of the XiX sequence approaches, of course, that of cw decoupling. This is illustrated in Fig. 3, which shows the same trace as Fig. 2a, extended to pulse widths of up to 150 rotor periods.

Numerical simulations of the XiX sequence, using a simple heteronuclear two-spin model, exhibit the same basic features as the experimental data. These results are shown in Fig. 2d. Unwanted ‘resonances’ similar to those in the experimental data are observed whenever the pulse

width matches multiples of a quarter of the rotor period. The calculations predict good decoupling whenever these conditions are avoided. The weaker minima at certain multiples of 1/24th of a rotor period are not reproduced by the numerical simulations. This can be attributed to the simplicity of the spin system which does not include homonuclear proton–proton couplings.

The occurrence of the deep ‘resonances’ at multiples of a quarter of the rotor period can be understood by regarding the XiX sequence as an example of a so-called CN_n^r sequence [6,14,15]. For this we identify a C element with the basic repeating unit of the XiX sequence, i.e., two phase-inverted pulses of width t_p each. At the positions of the minima ($t_p = n \cdot \tau_r/4$), the XiX sequence can then be identified with a sequence of the type $C2_n^0$. For these sequences, lowest-order average Hamiltonian considerations predict that heteronuclear dipolar interactions are reintroduced by interference of the pulse sequence with the MAS rotation. This explains the bad decoupling performance at the deep ‘resonances’ in Fig. 2. Further theoretical investigations of the XiX sequence are under way.

A comparison of spectra acquired under XiX and TPPM decoupling for different samples and under different experimental conditions is made in Fig. 4. Experimental spectra are shown for a CH group and a CH_2 group (in alanine and glycine, respectively). For each sample, MAS frequency, and rf-field amplitude, the performance of both TPPM and XiX decoupling was optimized experimentally as described above. For each pair of spectra shown here, it was carefully checked that the integrals of the resonance lines were identical within experimental uncertainty.

Fig. 4a shows the $^{13}C^\alpha$ line of alanine (CH group) at MAS frequencies of 30.03 and 20 kHz and at three different rf amplitudes under the two decoupling sequences. In all situations shown here, the height of the resonance line under optimized XiX decoupling is increased over the value found for TPPM. As mentioned already, the line width (FWHH) is very similar for both sequences, and the gain is primarily obtained by a sharpening of the broad ‘foot’ in the TPPM spectra. The strongest improvement of 29% is achieved at the

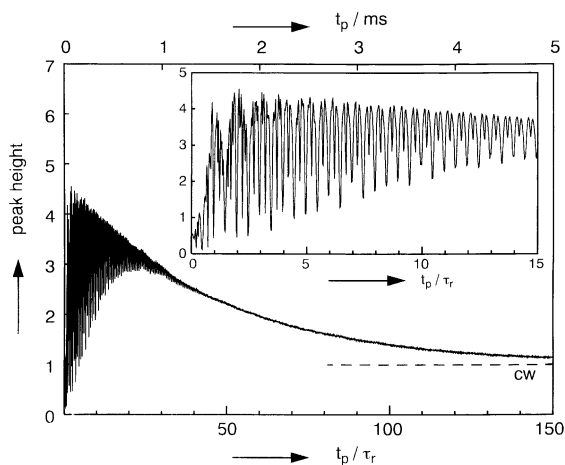


Fig. 3. Pulse-width dependence of XiX decoupling for t_p up to 5 ms ($150 \tau_r$). The line height of the C^α resonance of alanine is shown as a function of t_p at a MAS frequency of 30.03 kHz and a rf-field amplitude of 150 kHz (as in Fig. 2a). The line height is normalized to cw decoupling at the same rf-field amplitude, indicated by the horizontal dashed line. The inset shows the same data, but only up to 500 μs ($15 \tau_r$).

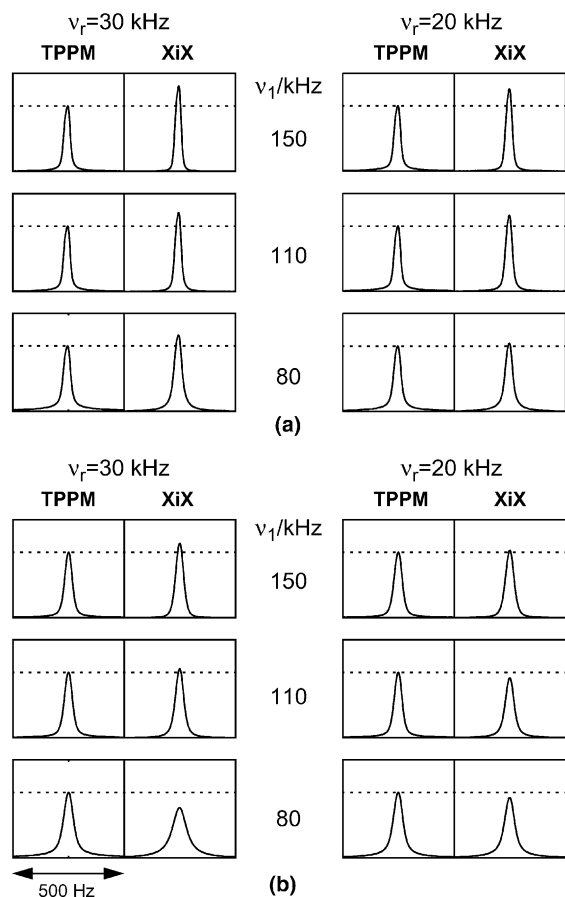


Fig. 4. The C^α resonances of (a) $2\text{-}^{13}\text{C}$ -alanine and (b) $2\text{-}^{13}\text{C}$ -glycine for TPPM and XiX decoupling at two different MAS frequencies and at three different rf-field amplitudes. For each spectrum, the parameters of the two decoupling sequences were adjusted to give maximum peak height.

highest rf-field amplitude of 150 kHz and at 30 kHz MAS. The relative merits of XiX, when compared to TPPM, thus seem to be best at high rf fields and rapid MAS. At high rf fields, however, XiX can outperform TPPM even at the relatively slow MAS frequency of 10 kHz (data not shown).

The behavior noticed for the CH group becomes more pronounced for the CH_2 group of glycine, as shown in Fig. 4b. Again, both TPPM and XiX were optimized. While under rapid MAS and high rf fields (e.g., $\nu_r = 30$ kHz and $\nu_1 = 150$ kHz) gains over TPPM are achieved by using XiX decoupling, TPPM offers advantages at lower rf fields and slower MAS.

It may be noted that all spectra in Fig. 4 were recorded immediately after the sequence parameters had been optimized. When these spectra were again recorded with the same parameters under even only slightly different conditions (e.g., after a very slight detuning of the probe), the advantages of the XiX sequences became more pronounced: while the signal under XiX decoupling was virtually unchanged, the line height under TPPM decoupling was usually reduced significantly due to slight changes in the rf-field strength.

The sensitivity of TPPM and XiX decoupling to such effects and to rf-field inhomogeneities can be compared by measuring the dependences of the peak height on the rf-field amplitude, while keeping all other parameters fixed. Fig. 5 shows this dependence for one particular set of parameters. These spectra were obtained from the CH group of alanine in a rotor whose sample volume was restricted to the central 1.5 mm along the rotor axis. The MAS frequency was 30 kHz. The TPPM performance had been optimized at an rf-

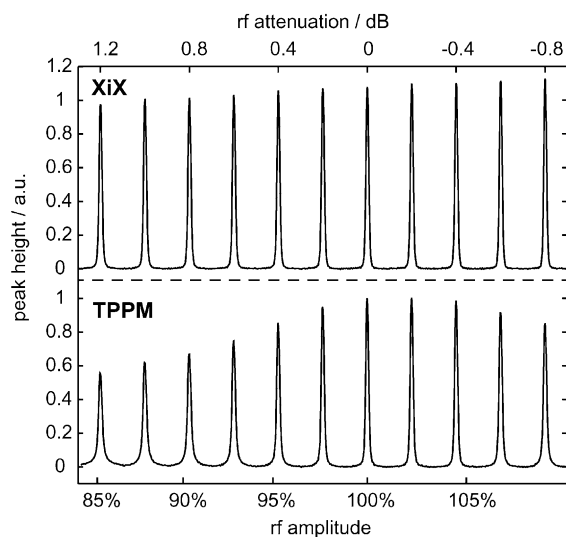


Fig. 5. Dependence of the C^α resonance of alanine on the rf-field amplitude for XiX (top) and TPPM decoupling (bottom). An amplitude of 100% (0 dB) corresponds to $\nu_1 = 130$ kHz, where both sequences were optimized. Only a weak dependence of the performance on the rf-field amplitude is observed in the case of XiX. A much stronger rf-field dependence is observed for TPPM, making TPPM more susceptible to rf-field inhomogeneity or amplifier instability.

field amplitude of $\nu_1 = 130$ kHz, yielding parameters $t_p = 3.7$ μ s and $\Delta\phi = 35^\circ$. At both higher and lower rf-field amplitudes, the performance of TPPM decoupling degrades significantly if these parameters are kept fixed. Optimization of the XiX sequence at $\nu_1 = 130$ kHz yielded an optimum pulse width of $t_p = 93.7$ μ s. Keeping this fixed, the dependence on the rf-field amplitude is much weaker than for TPPM. This illustrates once more the fact that the flip angle of the individual rf pulses is not a critical quantity in XiX decoupling.

As mentioned above, for obtaining optimum decoupling using TPPM it is required to optimize both the pulse width and the phase difference of the sequence. Predictions for the optimum values are difficult to make and, especially at higher MAS frequencies, TPPM becomes very sensitive to the precise setting of the parameters. The new XiX sequence, on the other hand, only has a single parameter, and, based on the MAS frequency, one can predict the location of the performance maxima quite well. As a rule of thumb, a good starting value for the pulse width when using XiX decoupling is $t_p = 1.85 \cdot \tau_r$ or $t_p = 2.85 \cdot \tau_r$. From these starting values a local optimization of the pulse width should be sufficient for obtaining a close-to-optimum performance.

Its simplicity allows modifications of the XiX sequence in several different directions. By making the two different pulses slightly unequal in either width or amplitude, e.g., a small effective transverse field can be added. The presence of the effective field turns out to significantly increase the performance for short pulse widths of less than a rotor period (results not shown). It is also possible to replace the ‘hard’ pulses of the XiX sequence by adiabatic inversion pulses. Promising preliminary results have been achieved with this modification.

4. Conclusions

Gains in peak height of up to 29% over TPPM were demonstrated for the XiX decoupling sequence. The gain in peak height is, in the samples investigated, mainly due to a sharpening of the

broad ‘foot’ that is observed when using TPPM or cw decoupling. In addition to a gain in resolution, application of the new sequence can lead to significant gains in sensitivity. When applied to typical organic or biological solids, the XiX sequence is best suited for high MAS frequencies (above ca. 20 kHz) and high rf fields (above ca. 100 kHz), even though gains over the known decoupling sequences have been observed in certain cases already at an MAS frequency of 10 kHz.

The decoupling sequence is easily set up and adjusted since it depends only on a single parameter, i.e., the pulse width t_p . As a good starting value, the pulse width can be adjusted to $t_p = 2.85 \cdot \tau_r$ and then optimized experimentally in a relatively narrow range ($\pm 0.1 \cdot \tau_r$). As the performance depends primarily only on the timing of the sequence relative to the sample rotation, transmitter instability, probe detuning or rf-field inhomogeneity do not critically affect the performance of the sequence.

Acknowledgements

Financial support by the Swiss National Science Foundation and the ETH Zurich is acknowledged. E.H. was supported by a post-doctoral fellowship of the Deutsche Forschungsgemeinschaft.

References

- [1] M. Mehring, *Principles of High Resolution NMR in Solids*, second ed., Springer, Berlin, 1983.
- [2] U. Haeberlen, *High Resolution NMR in Solids: Selective Averaging*, Academic Press, New York, 1976.
- [3] K. Schmidt-Rohr, H.W. Spiess, *Multidimensional Solid-State NMR and Polymers*, Academic Press, London, 1994.
- [4] A.E. Bennett, C.M. Rienstra, M. Auger, K.V. Lakshmi, R.G. Griffin, *J. Chem. Phys.* 103 (1995) 6951.
- [5] Z.H. Gan, R.R. Ernst, *Solid State NMR* 8 (1997) 153.
- [6] M. Eden, M.H. Levitt, *J. Chem. Phys.* 111 (1999) 1511.
- [7] Y. Yu, B.M. Fung, *J. Magn. Reson.* 130 (1998) 317.
- [8] B.M. Fung, A.K. Khitrin, K. Ermolaev, *J. Magn. Reson.* 142 (2000) 97.
- [9] K. Takegoshi, J. Mizokami, T. Terao, *Chem. Phys. Lett.* 341 (2001) 540.
- [10] M. Ernst, B.H. Meier, *Chem. Phys. Lett.* 348 (2001) 293.
- [11] S. Hediger, B.H. Meier, N.D. Kurur, G. Bodenhausen, R.R. Ernst, *Chem. Phys. Lett.* 223 (1994) 283.

- [12] S. Hediger, B.H. Meier, R.R. Ernst, *Chem. Phys. Lett.* 240 (1995) 449.
- [13] S. Smith, T. Levante, B.H. Meier, R.R. Ernst, *J. Magn. Reson. Ser. A* 106 (1994) 75.
- [14] Y.K. Lee, N.D. Kurur, M. Helmle, O.G. Johannessen, N.C. Nielsen, M.H. Levitt, *Chem. Phys. Lett.* 242 (1995) 304.
- [15] A. Brinkmann, M.H. Levitt, *J. Chem. Phys.* 115 (2001) 357.